Printed colorimetric chemosensor array on a 96-microwell paper substrate for metal ions in river water

Yui Sasaki†, Xiaojun Lyu† and Tsuyoshi Minami*

Institute of Industrial Science, The University of Tokyo, Tokyo, Japan

Here, we propose a printed 96-well microtiter paper-based chemosensor array device (PCSAD) to simultaneously detect metal ions for river water assessment. Colorimetric chemosensors for metal ions have been designed based on molecular self-assembly using off-the-shelf catechol dyes and a phenylboronic acid (PBA) derivative. The colorimetric self-assembled chemosensors consisting of catechol dyes and a PBA derivative on a 96-well microtiter paper substrate demonstrated various color changes according to the disassembly of the ensembles by the addition of nine types of metal ions. An in-house-made algorithm was used to automate imaging analysis and extract color intensities at seven types of color channels from a captured digital image, allowing for rapid data processing. The obtained information-rich inset data showed fingerprint-like colorimetric responses and was applied to the qualitative and quantitative pattern recognition of metal ions using chemometric techniques. The feasibility of the 96-well microtiter PCSAD for environmental assessment has been revealed by the demonstration of a spike-and-recovery test against metal ions in a river water sample.

Introduction

With increasing attention paid to high-throughput chemical analysis, computational methods are widely utilized owing to their powerful data processability (Jurs et al., 2000; Anzenbacher et al., 2010; Li et al., 2019). In this regard, chemical sensor platforms for the simultaneous detection of multiple analytes, which are referred to as sensor arrays (Dickinson et al., 1996; Lavigne et al., 1998; Vlasov and Legin, 1998; Rakow and Suslick, 2000), have been vigorously developed thus far. Chemosensor arrays are analytical tools for pattern recognition at the molecular levels, which enable the visualization of molecular recognition information through optical changes upon capturing analytes (Kitamura et al., 2009; Peveler et al., 2016; Sasaki et al., 2021a). Based on the inherent cross-reactivities of artificial receptors (Gardner, 1991), chemosensors in an array display a fingerprint-like response pattern according to the different types of analytes and their concentrations (Anzenbacher et al., 2010; Sasaki et al., 2021a). Therefore, qualitative and quantitative chemical information at the molecular level can be analyzed by data processing of the optical fingerprint-like response pattern (Huang et al., 2013; Sener et al., 2014; Xu et al., 2014;

Hwang et al., 2015), allowing for accurate sensing, even in real samples (Palacios et al., 2008; Li J. et al., 2020; Li Y. et al., 2020; Bowyer et al., 2022).

Molecular recognition information on chemosensor arrays in solution is conventionally acquired by spectrophotometers, whereas the applicability to on-site analysis is limited by solution-based sensing systems (Sasaki et al., 2021b; Sasaki et al., 2022). Hence, we have focused on chemosensor arrays embedded in solid-state sensor devices to establish easy-to-use chemical sensor devices (Xu and Bonizzoni, 2020; Lyu et al., 2021; Zhang et al., 2021; Lyu et al., 2022). Paper is a representative solid-state substrate in the field of analytical chemistry, and its superior processability has facilitated the development of printed paper-based analytical devices (Martinez et al., 2010; Feng et al., 2013; Yamada et al., 2015; Karita and Kaneta, 2016; Tan et al., 2022). Disposable paper-based analytical devices have been applied to real-sample analysis (e.g., river water) in combination with portable recording apparatuses for environmental assessment (Chen et al., 2014; Karita and Kaneta, 2016; Kung et al., 2019; Liu et al., 2019), while simultaneous discrimination of multiple metal ions and quantitative detection by solid-state portable sensor devices in river water samples is still at the frontier. Thus far, we designed a paper-based chemosensor array device (PCSAD) for the simultaneous detection of multiple metal ions based on molecular self-assembly.

The ability of chemosensor arrays to perform classification and prediction relies on the quality of the inset data, although data processing using powerful statistical methods can be applied. This indicates that an optimal design of chemosensors is required to obtain an information-rich data matrix for pattern recognition (Sasaki et al., 2020; Sasaki et al., 2021a). Such an information-rich dataset is conventionally acquired by collecting various types of chemosensors possessing different optical characteristics to increase the variables that correspond to wavelength, absorbance, and fluorescence intensity. Considering contribution of each chemosensor to pattern recognition (Liu et al., 2013), the sophisticated design of chemosensors that provide drastic optical changes is more important than the number of chemosensors for obtaining information-rich datasets (Sasaki et al., 2020). A molecular self-assembled system through non-covalent bonds exhibits inherent reversible behavior based on the assembly and disassembly of building blocks. By utilizing the unique features of self-assemblies to chemosensors, the optical responses of the chemosensors can be manipulated through competitive responses among the building blocks of the chemosensors and analytes (Nguyen and Anslyn, 2006; Sedgwick et al., 2021). In particular, the optical contrast derived produced by the reversible molecular self-assemblies is significant for imaging analysis on the PCSADs. This indicates that chemosensor designs based on non-covalent chemistry are promising for establishing the PCSADs for real-sample analysis. Phenylboronic acid (PBA) forms a boronate ester with cis-diols, and the attractive reversibility of PBA derivatives can be utilized as a manipulator of a catechol dye for tuning optical properties (Kubo et al., 2005; Sasaki et al., 2017). The optical profiles of catechol dyes are manipulated by boronate esterification (Springsteen and Wang, 2001; Tomsho and Benkovic, 2012) causing blueshifts because of the changes in the negative charge states of the catechol dyes at neutral pH conditions (Tomsho and Benkovic, 2012; Sasaki et al., 2017). Upon the addition
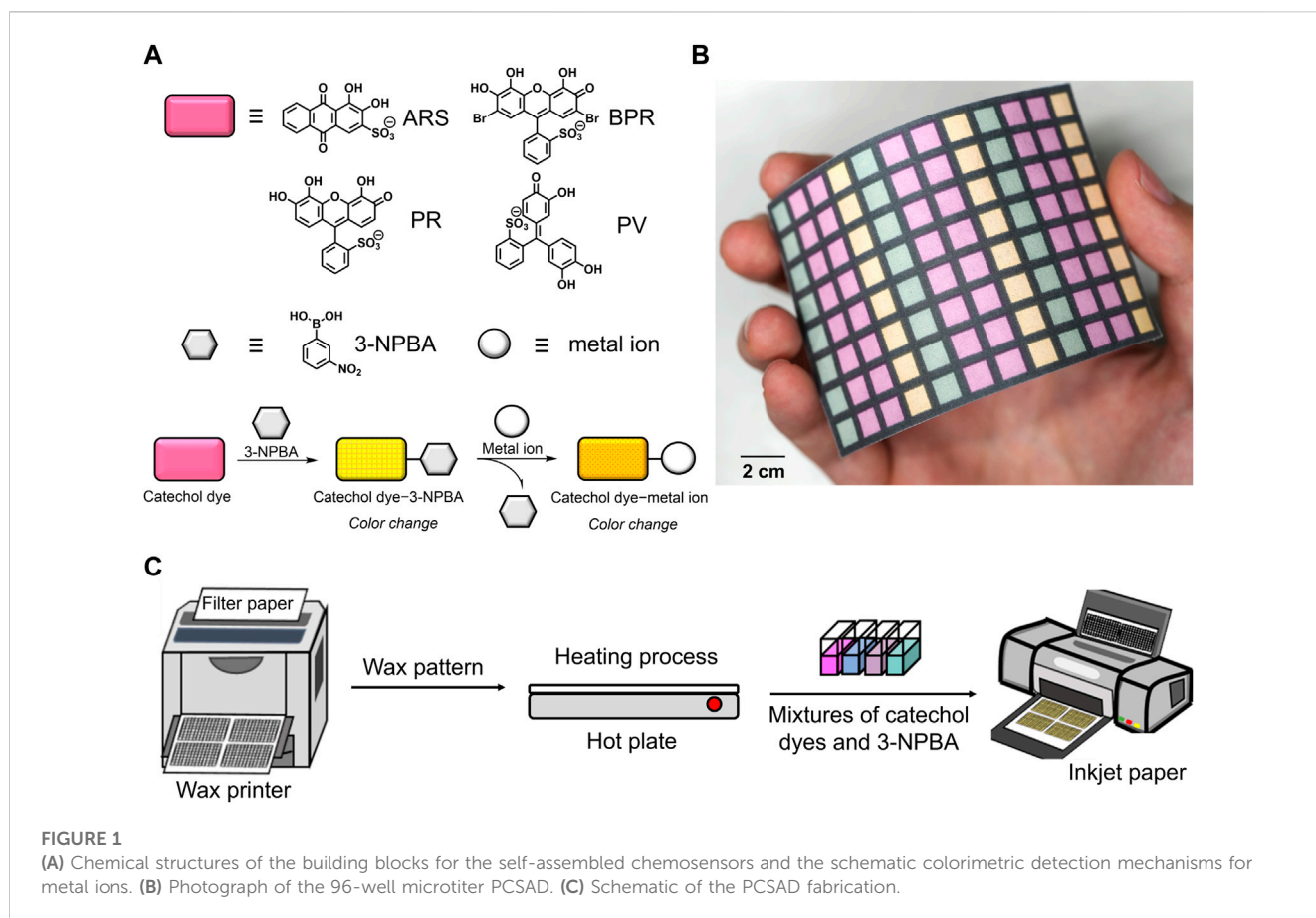
of the target metal ions to the complex of the catechol dye and PBA derivative, colorimetric changes are induced by the release of the PBA derivative from the boronate esters accompanied by the complexation of the catechol dyes and metal ions (Kaushik et al., 2015; Lin et al., 2018). The coordination between the catechol dyes and target metal ions promotes deprotonation of the catechol dyes (Zhang et al., 2007), whereby redshifts can be observed (Sasaki et al., 2017). In this study, four types of catechol dyes [i.e., alizarin red S (ARS), bromopyrogallol red (BPR), pyrogallol red (PR), and pyrocatechol violet (PV)] and 3-nitrophenylboronic acid (3-NPBA) (Sasaki et al., 2019) were employed as the building blocks for the colorimetric chemosensors against nine metal ions (i.e., Cu^{2+}, Zn^{2+}, Ni^{2+}, Cd^{2+}, Al^{3+}, Pb^{2+}, Co^{2+}, Ca^{2+}, and Mg^{2+}) (Figure 1). In this regard, the nitro group of 3-NPBA enhances the Lewis-acidity of boronic acid, facilitating boronate esterification with catechol dyes under neutral pH conditions (Sasaki et al., 2017; Sasaki et al., 2019). For example, boron–nitrogen (B–N) interactions have been widely used to form boronate esters with diol units, while a single B–N interaction alone was insufficient to tune the color profiles of dyes through complexation with PBA derivatives (Koumoto et al., 1998). Specifically, the role of the electron-withdrawing nitro group is more significant than that of the B-N interaction (Koumoto et al., 1998).

During the device fabrication, an office wax printer was used to dispense the hydrophobic barrier onto the filter paper to avoid leakage of the target solutions (Figure 1). Chemosensor solutions made of 3-NPBA and catechol dyes were injected into a 96-well microtiter PCSAD using an office inkjet printer to obtain solid-state detection portions (Figure 1). Upon drop-casting the metal ion solutions onto each well, various color changes were observed and rapidly scanned using a flatbed scanner. The obtained digital color images were automatically analyzed by an in-house-made algorithm, followed by the construction of a data matrix containing color intensities in different color channels. We evaluated the detectability of the manufactured 96-well microtiter PCSAD and further applied it to the regression analysis of metal ions in a river water sample using pattern recognition techniques.

Materials and methods

Reagents

All reagents used for device fabrication and sensing were utilized without further pre-treatment. ARS, a commercially available river sample with trace elements in river water (Elevated Level, NMIJ CRM 7202-c, Supplementary Table S1), and iron(III) nitrate enneahydrate (Fe^{3+}) were obtained from FUJIFILM Wako Pure Chemical Co., Ltd. The target metal ions including cobalt(II) perchlorate hexahydrate (Co^{2+}), calcium perchlorate tetrahydrate (Ca^{2+}), lead(II) perchlorate trihydrate (Pb^{2+}), cadmium perchlorate hydrate (Cd^{2+}), nickel(II) perchlorate hexahydrate (Ni^{2+}), copper(II) perchlorate hexahydrate (Cu^{2+}), magnesium perchlorate hexahydrate (Mg^{2+}), aluminum perchlorate non-ahydrate (Al^{3+}), mercury(II) perchlorate hydrate (Hg^{2+}), and zinc perchlorate hexahydrate (Zn^{2+}) were purchased from Sigma-Aldrich. The building blocks of the chemosensors purchased from Tokyo Chemical Industry Co., Ltd. were 3-NPBA, BPR, PR, and PV. A buffer material purchased from DOJINDO was 4-(2-hydroxyethyl)-

FIGURE 1
(A) Chemical structures of the building blocks for the self-assembled chemosensors and the schematic colorimetric detection mechanisms for metal ions. **(B)** Photograph of the 96-well microtiter PCSAD. **(C)** Schematic of the PCSAD fabrication.

1-piperazineethanesulfonic acid (HEPES). All aqueous solutions were prepared using Milli-Q water (18.2 Ω cm).

Device fabrication

Based on our previous reports on the colorimetric self-assembled chemosensor arrays using off-the-shelf materials (Sasaki et al., 2017) and the fabrication of paper-based sensor devices (Sasaki et al., 2021b; Lyu et al., 2021), a colorimetric PCSAD for metal ions was designed. A filter paper adjusted to A4 size (Whatman grade 1, GE Healthcare, Buckinghamshire, UK) was used as the solid-state substrate for PCSAD. Hydrophobic barriers were fabricated on the smooth front side of the filter paper using an office wax printer (ColorQube 8580, Xerox). A 96-well plate pattern was printed with a square shape (5 mm^2 × 5 mm^2), and the gap between each well was set to 2 mm. The printed pattern was annealed at 150°C for 60 s on a hot plate (NHS-450ND, NISSIN Co.). The printed wax melts during the annealing process, and hydrophobic barriers were formed by the penetration of the melted wax into the filter paper. The filter paper substrate was cooled to 25°C. The self-assembled complexes, which were evaluated using a UV-vis spectrophotometer in a previous study (Sasaki et al., 2017), were applied to printing inks for device fabrication in this assay. Therefore, a HEPES solution (50 mM, pH 7.4) containing catechol dyes (2 mM) and 3-NPBA (30 mM) was dispensed into the wells

with five printing cycles using an inkjet printer (PIXUS TS203, Canon Inc.). Moreover, the target metal ions contained in the HEPES buffer solution (50 mM) or the mixture of river water and HEPES (1:1, v/v) (10 μL) adjusted to pH 7.4 were pipetted onto each well and then dried at room temperature under dark conditions. The optical responses of the 96-well microtiter PCSAD were quickly recorded using a flatbed scanner (CanoScan 9000F Mark II, Canon Inc.) with a scan resolution of 600 dpi.

Data acquisition and analysis

An in-house-made algorithm constructed using MathWorks MATLAB 2022 was applied to the imaging analysis of the captured images of the color response. The entire image was first automatically divided into image slices that contained two control areas and ten repetition areas, while the wax backgrounds (i.e., black area in the PCSAD) were eliminated by the morphological detection using the red channel. Thus, the 96-wells of the PCSAD were individually separated for further imaging analyses. In this analysis, the color responses on the wells with added metal ions (i.e., the sensing area) were evaluated based on the colorimetric differences between the sensing and control areas (i.e., wells without added metal ions). A data matrix was constructed using the color intensities of the four chemosensors at seven optical channels with RGB (i.e., red, green, and blue color channels), grayscale, and YC_bC_r
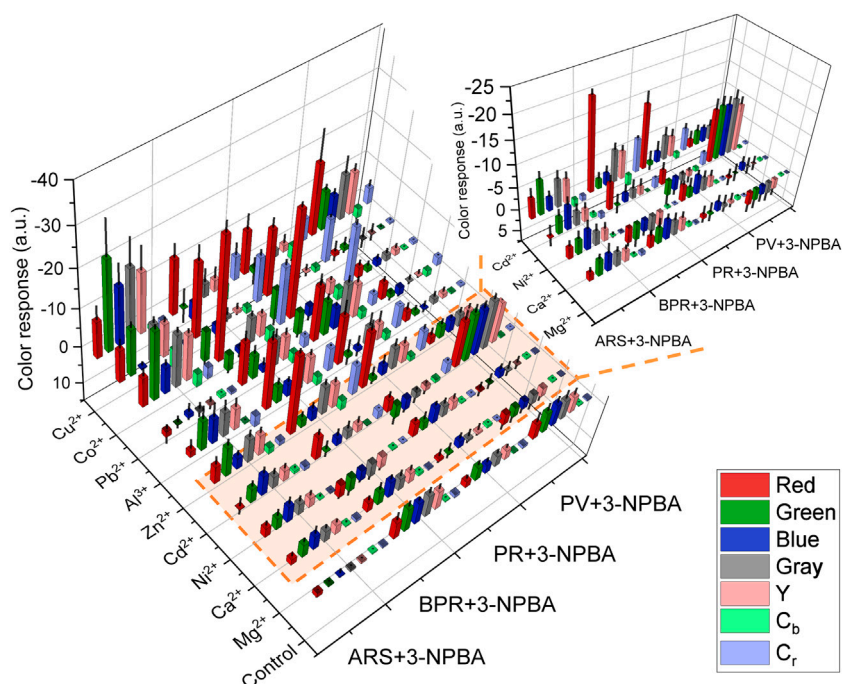
FIGURE 2
Color response profile of the 96-well microtiter PCSAD upon adding target metal ions (50 µM) in a HEPES buffer solution (50 mM) at pH 7.4.

(i.e., Y for the luma component and, C_b and C_r for blue- and red-difference chroma components), indicating 28 variables. Further, Student's t-test was used to remove two outliers among the ten repetitions for each metal ion. Linear discriminant analysis (LDA) for the qualitative and semi-quantitative assays was performed using SYSTAT 13 without any further data treatment. Support vector machine (SVM) with Solo 9.0. performed a quantitative analysis of spike-and-recovery tests. The mean relative error values of the multisensory system (Oleneva et al., 2019) was evaluated to determine the limit of detection (LOD).

Results and discussion

The 96-well microtiter PCSAD exhibited various color changes with different types of metal ions, which stemmed from the different binding affinities of the catechol dyes to the analytes (Kubo et al., 2005; Sasaki et al., 2017). As shown in Figure 2, the color intensity profile of the 96-well microtiter PCSAD obtained by imaging analysis demonstrated a fingerprint-like colorimetric response pattern against the nine metal ions, implying its high potential for pattern recognition-driven chemosensing. Therefore, a paper-based chemosensor array system was applied to the simultaneous discrimination of nine types of metal ions using LDA, enabling the classification of clusters and decreasing the multi-dimensional inset data for pattern recognition (Anzenbacher et al., 2010).

Figure 3 and Supplementary Figure S1 show the canonical score plot containing ten clusters (nine metal ions and a control) with eight repetition datasets for each analyte. The LDA result
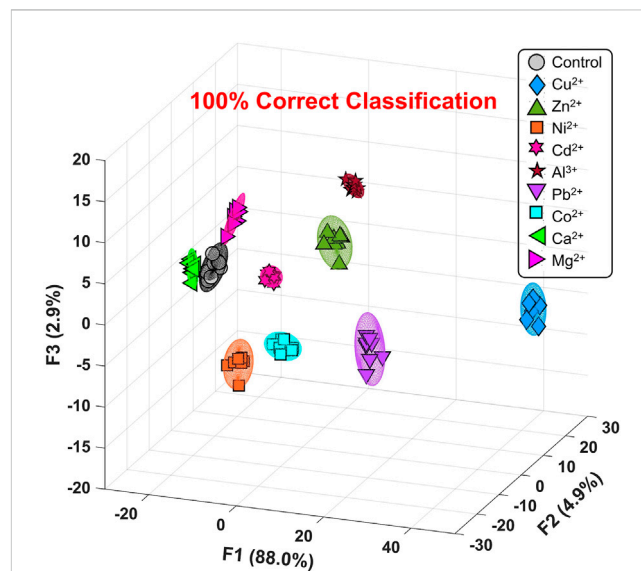

FIGURE 3
Canonical score plot by LDA for the qualitative assay against nine types of metal ions (50 µM) in a HEPES buffer solution (50 mM, at pH 7.4) with 95% confidence ellipsoids. All clusters with eight repetitive datasets for each analyte were distributed with 100% correct classification.

suggested the success of the discrimination of nine metal ions without misclassification (Supplementary Table S1). In contrast, the PCSAD unsuccessfully discriminated Fe^{3+} and Hg^{2+}, which
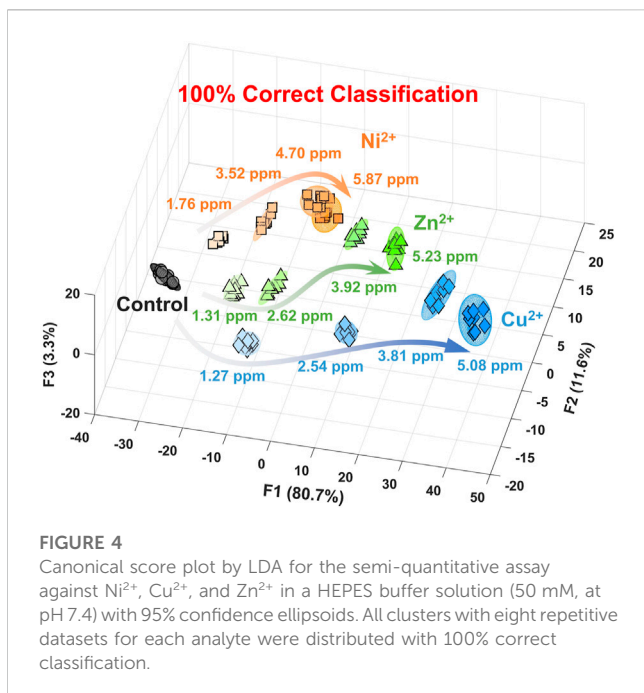
FIGURE 4
Canonical score plot by LDA for the semi-quantitative assay against Ni²⁺, Cu²⁺, and Zn²⁺ in a HEPES buffer solution (50 mM, at pH 7.4) with 95% confidence ellipsoids. All clusters with eight repetitive datasets for each analyte were distributed with 100% correct classification.

determined to be 0.15, 0.17, and 0.28 ppm, respectively (Supplementary Figure S3). The estimated values represented the sufficient detectability judging from the values of environmental quality standards (Verschoor et al., 2011).

Finally, we demonstrated a spike and recovery test for Ni²⁺, Cu²⁺, and Zn²⁺ in a river water sample using SVM, which is a powerful chemometric algorithm for building a linear calibration line in a complicated response pattern (Hamel, 2009; Minami et al., 2012). The calibration datasets (gray squares) for each target metal ion were respectively obtained in 0–100 μM range of the target metal ions in a HEPES buffer (50 mM, pH 7.4). As shown in Figure 5, the prediction datasets for Zn²⁺ (green circles) and Cu²⁺ (blue circles) are correctly distributed on the calibration lines with a low root-mean-square error of prediction. However, the unknown concentrations of Ni²⁺ in the river water samples were not successfully predicted (Supplementary Figure S4) because of the weaker response of the 96-well microtiter PCSAD to Ni²⁺ than to Cu²⁺ and Zn²⁺ as shown in the color intensity profile (Figure 2). Furthermore, the recovery rates for Zn²⁺ at 10, 20, and 30 μM and Cu²⁺ at 20, 40, and 60 μM were estimated to be 89%–125% (Supplementary Table S4). The proposed PCSAD combined with pattern
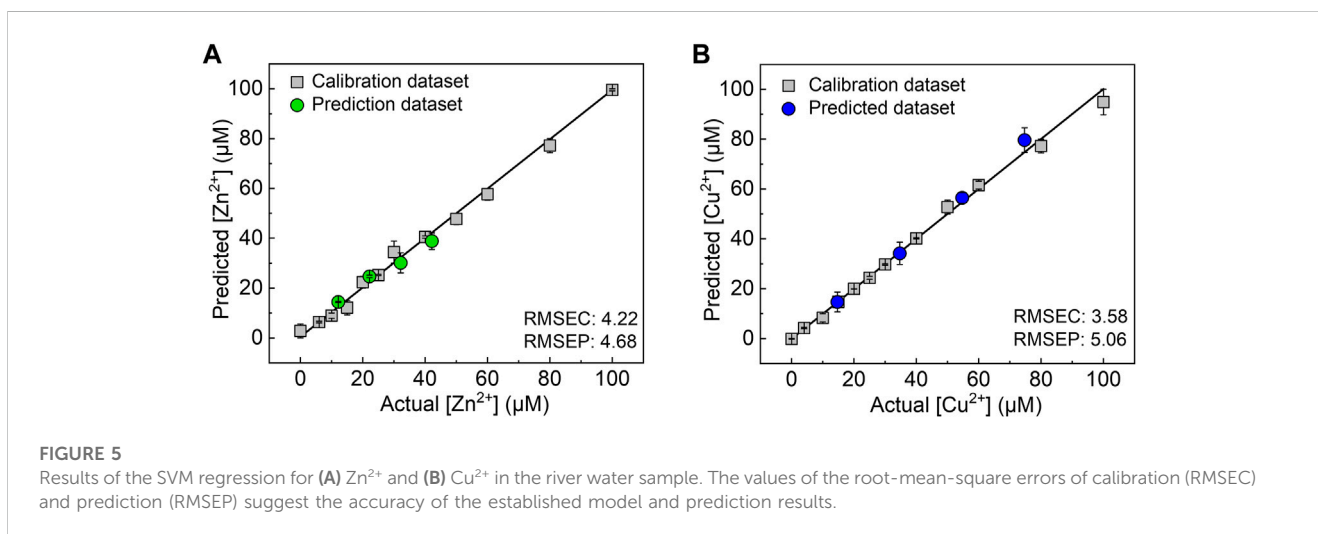

FIGURE 5
Results of the SVM regression for (A) Zn²⁺ and (B) Cu²⁺ in the river water sample. The values of the root-mean-square errors of calibration (RMSEC) and prediction (RMSEP) suggest the accuracy of the established model and prediction results.

was probably due to the hydrolysis of the metal ions at neutral pH conditions. Moreover, the printed 96-well microtiter PCSAD was used to perform a semi-quantitative assay to simultaneously evaluate the discrimination power of analytes and their concentrations. The selected three species (i.e., Ni²⁺, Cu²⁺, and Zn²⁺) could have an antagonistic effect on the growth of microorganisms in ecosystems, whereby the quantitative detection of the levels of the three metal ions is essential from the perspective of environmental assessment (Payette and Yamamoto, 2011). The LDA results in Figure 4 show a concentration-dependent cluster distribution for all the analytes, indicating the accuracy of the manufactured 96-well microtiter PCSAD (Supplementary Table S2). Moreover, the LoD of the 96-well PCSAD for Cu²⁺, Zn²⁺, and Ni²⁺ was

recognition accurately predicted unknown concentrations of metal ions in the river water samples, suggesting the usability of the proposed method for the accurate and sensitive detection of metal ions in environmental samples.

Conclusion

In this study, we designed a colorimetric chemosensor array on a 96-well microtiter paper-based device for metal ion detection. The self-assembled chemosensor array was designed to obtain a unique optical contrast upon the addition of metal ions, which was derived from a competitive assay. In this regard, the reversibility of the colorimetric boronate esters contributed to an increase in the

optical response patterns during the assembly and disassembly with catechol dyes. Indeed, chemosensors comprising catechol dyes and 3-NPBA as printing inks demonstrated various color changes upon the addition of nine metal ions, allowing pattern recognition-driven chemical sensing through the fingerprinting-like colorimetric response on paper. Hence, the 96-well microtiter PCSAD succeeded in the simultaneous discrimination of nine metal ions with 100% correct classification. In the semi-quantitative assay of Ni^{2+}, Cu^{2+}, and Zn^{2+}, a concentration-dependent cluster distribution was observed using LDA. Finally, the applicability of the 96-well microtiter PCSAD for metal ion assessment in river water was evaluated using a spike-and-recovery test. The estimated recovery rates for metal ions in the river water sample (89%–125%) suggest its potential as a facile paper-based analytical device enabling both qualitative and quantitative analysis of real samples. Although further improvements in the accuracy of the sensor devices are required, we believe that an appropriate sensor design based on molecular recognition chemistry could create new avenues for the realization of supramolecular analytical devices.

Data availability statement

The original contributions presented in the study are included in the article/Supplementary Material, further inquiries can be directed to the corresponding author.

Author contributions

The manuscript was written by YS and XL. XL performed device fabrication, sensing, and data analysis. TM conceived the entire project.

Conflict of interest

The authors declare that the research was conducted in the absence of any commercial or financial relationships that could be construed as a potential conflict of interest.

Publisher's note

All claims expressed in this article are solely those of the authors and do not necessarily represent those of their affiliated organizations, or those of the publisher, the editors and the reviewers. Any product that may be evaluated in this article, or claim that may be made by its manufacturer, is not guaranteed or endorsed by the publisher.

Supplementary material

The Supplementary Material for this article can be found online at: https://www.frontiersin.org/articles/10.3389/fchem.2023.1134752/full#supplementary-material

References

Anzenbacher, P., Jr. Lubal, P., Buček, P., Palacios, M. A., and Kozelkova, M. E. (2010). A practical approach to optical cross-reactive sensor arrays. *Chem. Soc. Rev.* 39, 3954–3979. doi:10.1039/B926220M

Bowyer, A. A., Mai, A. D., Guo, H., and New, E. J. (2022). A pH-based single-sensor array for discriminating metal ions in water. *Chem. Asian J.* 17, e202200204. doi:10.1002/asia.202200204

Chen, G.-H., Chen, W.-Y., Yen, Y.-C., Wang, C.-W., Chang, H.-T., and Chen, C.-F. (2014). Detection of mercury(II) ions using colorimetric gold nanoparticles on paper-based analytical devices. *Anal. Chem.* 86, 6843–6849. doi:10.1021/ac5008688

Dickinson, T. A., White, J., Kauer, J. S., and Walt, D. R. (1996). A chemical-detecting system based on a cross-reactive optical sensor array. *Nature* 382, 697–700. doi:10.1038/382697a0

Feng, L., Li, X., Li, H., Yang, W., Chen, L., and Guan, Y. (2013). Enhancement of sensitivity of paper-based sensor array for the identification of heavy-metal ions. *Anal. Chim. Acta* 780, 74–80. doi:10.1016/j.aca.2013.03.046

Gardner, J. W. (1991). Detection of vapours and odours from a multisensor array using pattern recognition Part 1. Principal component and cluster analysis. *Sens. Actuators B Chem.* 4, 109–115. doi:10.1016/0925-4005(91)80185-M

Hamel, L. H. (2009). *Knowledge discovery with support vector machines*. Hoboken, USA: Wiley.

Huang, Y., Li, F., Qin, M., Jiang, L., and Song, Y. (2013). A multi-stopband photonic-crystal microchip for high-performance metal-ion recognition based on fluorescent detection. *Angew. Chem. Int. Ed.* 52, 7296–7299. doi:10.1002/anie.201302311

Hwang, I. H., Hong, K. I., Jeong, K. S., and Jang, W. D. (2015). Carbazole-based molecular tweezers as platforms for the discrimination of heavy metal ions. *RSC Adv.* 5, 1097–1102. doi:10.1039/c4ra13221a

Jurs, P. C., Bakken, G. A., and Mcclelland, H. E. (2000). Computational methods for the analysis of chemical sensor array data from volatile analytes. *Chem. Rev.* 100, 2649–2678. doi:10.1021/cr9800964

Karita, S., and Kaneta, T. (2016). Chelate titrations of Ca^{2+} and Mg^{2+} using microfluidic paper-based analytical devices. *Anal. Chim. Acta* 924, 60–67. doi:10.1016/j.aca.2016.04.019

Kaushik, R., Kumar, P., Ghosh, A., Gupta, N., Kaur, D., Arora, S., et al. (2015). Alizarin red S–zinc(ii) fluorescent ensemble for selective detection of hydrogen sulphide and assay with an H_2S donor. *RSC Adv.* 5, 79309–79316. doi:10.1039/C5RA11901D

Kitamura, M., Shabbir, S. H., and Anslyn, E. V. (2009). Guidelines for pattern recognition using differential receptors and indicator displacement assays. *J. Org. Chem.* 74, 4479–4489. doi:10.1021/jo900433j

Koumoto, K., Takeuchi, M., and Shinkai, S. (1998). Design of a visualized sugar sensing system utilizing a boronic acid-azopyridine interaction. *Supramol. Chem.* 9, 203–210. doi:10.1080/10610279808034988

Kubo, Y., Ishida, T., Kobayashi, A., and James, T. D. (2005). Fluorescent alizarin–phenylboronic acid ensembles: Design of self-organized molecular sensors for metal ions and anions. *J. Mater. Chem.* 15, 2889–2895. doi:10.1039/B501243K

Kung, C.-T., Hou, C.-Y., Wang, Y.-N., and Fu, L.-M. (2019). Microfluidic paper-based analytical devices for environmental analysis of soil, air, ecology and river water. *Sens. Actuators B Chem.* 301, 126855. doi:10.1016/j.snb.2019.126855

Lavigne, J. J., Savoy, S., Clevenger, M. B., Ritchie, J. E., McDoniel, B., Yoo, S.-J., et al. (1998). Solution-based analysis of multiple analytes by a sensor array: Toward the

development of an "electronic tongue". *J. Am. Chem. Soc.* 120, 6429–6430. doi:10.1021/ja9743405

Li, J., Cheng, Q., Huang, H., Li, M., Yan, S., Li, Y., et al. (2020). Sensitive chemical sensor array based on nanozymes for discrimination of metal ions and teas. *Luminescence* 35, 321–327. doi:10.1002/bio.3730

Li, Y., Hou, J., Zhou, H., Jia, M., Chen, S., Huang, H., et al. (2020). A fluorescence sensor array based on perylene probe monomer-excimer emission transition for the highly efficient differential sensing of metal ions and drinking waters. *Sens. Actuators B Chem.* 319, 128212. doi:10.1016/j.snb.2020.128212

Li, Z., Askim, J. R., and Suslick, K. S. (2019). The optoelectronic nose: Colorimetric and fluorometric sensor arrays. *Chem. Rev.* 119, 231–292. doi:10.1021/acs.chemrev.8b00226

Lin, Z.-Y., Xue, S.-F., Chen, Z.-H., Han, X.-Y., Shi, G., and Zhang, M. (2018). Bioinspired copolymers based nose/tongue-mimic chemosensor for label-free fluorescent pattern discrimination of metal ions in biofluids. *Anal. Chem.* 90, 8248–8253. doi:10.1021/acs.analchem.8b01769

Liu, Q., Lin, Y., Xiong, J., Wu, L., Hou, X., Xu, K., et al. (2019). Disposable paper-based analytical device for visual speciation analysis of Ag(I) and silver nanoparticles (AgNPs). *Anal. Chem.* 91, 3359–3366. doi:10.1021/acs.analchem.8b04609

Liu, Y., Minami, T., Nishiyabu, R., Wang, Z., and Anzenbacher, P., Jr. (2013). Sensing of carboxylate drugs in urine by a supramolecular sensor array. *J. Am. Chem. Soc.* 135, 7705–7712. doi:10.1021/ja4015748

Lyu, X., Hamedpour, V., Sasaki, Y., Zhang, Z., and Minami, T. (2021). 96-Well microtiter plate made of paper: A printed chemosensor array for quantitative detection of saccharides. *Anal. Chem.* 93, 1179–1184. doi:10.1021/acs.analchem.0c04291

Lyu, X., Sasaki, Y., Ohshiro, K., Tang, W., Yuan, Y., and Minami, T. (2022). Printed 384-well microtiter plate on paper for fluorescent chemosensor arrays in food analysis. *Chem. Asian J.* 17, e202200479. doi:10.1002/asia.202200479

Martinez, A. W., Phillips, S. T., Whitesides, G. M., and Carrilho, E. (2010). Diagnostics for the developing world: Microfluidic paper-based analytical devices. *Anal. Chem.* 82, 3–10. doi:10.1021/ac9013989

Minami, T., Esipenko, N. A., Zhang, B., Kozelkova, M. E., Isaacs, L., Nishiyabu, R., et al. (2012). Supramolecular sensor for cancer-associated nitrosamines. *J. Am. Chem. Soc.* 134, 20021–20024. doi:10.1021/ja3102192

Nguyen, B. T., and Anslyn, E. V. (2006). Indicator-displacement assays. *Coord. Chem. Rev.* 250, 3118–3127. doi:10.1016/j.ccr.2006.04.009

Oleneva, E., Khaydukova, M., Ashina, J., Yaroshenko, I., Jahatspanian, I., Legin, A., et al. (2019). A simple procedure to assess limit of detection for multisensor systems. *Sensors* 19, 1359. doi:10.3390/s19061359

Palacios, M. A., Wang, Z., Montes, V. A., Zyryanov, G. V., and Anzenbacher, P., Jr. (2008). Rational design of a minimal size sensor array for metal ion detection. *J. Am. Chem. Soc.* 130, 10307–10314. doi:10.1021/ja802377k

Payette, J. N., and Yamamoto, H. (2011). Borate and boronic acid derivatives as catalysts in organic synthesis, in *Boronic acids* Editor D. G. Hall 2 ed (Hoboken, USA: Wiley), 551–590.

Peveler, W. J., Yazdani, M., and Rotello, V. M. (2016). Selectivity and specificity: Pros and cons in sensing. *ACS Sens.* 1, 1282–1285. doi:10.1021/acssensors.6b00564

Rakow, N. A., and Suslick, K. S. (2000). A colorimetric sensor array for odour visualization. *Nature* 406, 710–713. doi:10.1038/35021028

Sasaki, Y., Kojima, S., Hamedpour, V., Kubota, R., Takizawa, S., Yoshikawa, I., et al. (2020). Accurate chiral pattern recognition for amines from just a single chemosensor. *Chem. Sci.* 11, 3790–3796. doi:10.1039/D0SC00194E

Sasaki, Y., Kubota, R., and Minami, T. (2021a). Molecular self-assembled chemosensors and their arrays. *Coord. Chem. Rev.* 429, 213607. doi:10.1016/j.ccr.2020.213607

Sasaki, Y., Lyu, X., Tang, W., Wu, H., and Minami, T. (2022). Supramolecular optical sensor arrays for on-site analytical devices. *J. Photochem. Photobiol. C* 51, 100475. doi:10.1016/j.jphotochemrev.2021.100475

Sasaki, Y., Lyu, X., Zhou, Q., and Minami, T. (2021b). Indicator displacement assay-based chemosensor arrays for saccharides using off-the-shelf materials toward simultaneous on-site detection on paper. *Chem. Lett.* 50, 987–995. doi:10.1246/cl.200962

Sasaki, Y., Minamiki, T., Tokito, S., and Minami, T. (2017). A molecular self-assembled colourimetric chemosensor array for simultaneous detection of metal ions in water. *Chem. Commun.* 53, 6561–6564. doi:10.1039/C7CC03218H

Sasaki, Y., Zhang, Z., and Minami, T. (2019). A saccharide chemosensor array developed based on an indicator displacement assay using a combination of commercially available reagents. *Front. Chem.* 7, 49. doi:10.3389/fchem.2019.00049

Sedgwick, A. C., Brewster, J. T., Wu, T., Feng, X., Bull, S. D., Qian, X., et al. (2021). Indicator displacement assays (IDAs): The past, present and future. *Chem. Soc. Rev.* 50, 9–38. doi:10.1039/C9CS00538B

Sener, G., Uzun, L., and Denizli, A. (2014). Colorimetric sensor array based on gold nanoparticles and amino acids for identification of toxic metal ions in water. *ACS Appl. Mater. Interfaces.* 6, 18395–18400. doi:10.1021/am5071283

Springsteen, G., and Wang, B. (2001). Alizarin Red S. as a general optical reporter for studying the binding of boronic acids with carbohydrates. *Chem. Commun.* 1608–1609. doi:10.1039/B104895N

Tan, W., Zhang, L., Jarujamrus, P., Doery, J. C. G., and Shen, W. (2022). Improvement strategies on colorimetric performance and practical applications of Paper-based analytical devices. *Microchem. J.* 180, 107562. doi:10.1016/j.microc.2022.107562

Tomsho, J. W., and Benkovic, S. J. (2012). Elucidation of the mechanism of the reaction between phenylboronic acid and a model diol, alizarin red S. *J. Org. Chem.* 77, 2098–2106. doi:10.1021/jo202250d

Verschoor, A. J., Vink, J. P. M., de Snoo, G. R., and Vijver, M. G. (2011). Spatial and temporal variation of watertype-specific No-effect concentrations and risks of Cu, Ni, and Zn. *Environ. Sci. Technol.* 45, 6049–6056. doi:10.1021/es2007963

Vlasov, Y., and Legin, A. (1998). Non-selective chemical sensors in analytical chemistry: From "electronic nose" to "electronic tongue". *Fresenius J. Anal. Chem.* 361, 255–260. doi:10.1007/s002160050875

Xu, W., Ren, C., Teoh, C. L., Peng, J., Gadre, S. H., Rhee, H.-W., et al. (2014). An artificial tongue fluorescent sensor array for identification and quantitation of various heavy metal ions. *Anal. Chem.* 86, 8763–8769. doi:10.1021/ac501953z

Xu, Y., and Bonizzoni, M. (2020). Disposable paper strips for carboxylate discrimination. *Analyst* 145, 3505–3516. doi:10.1039/D0AN00137F

Yamada, K., Henares, T. G., Suzuki, K., and Citterio, D. (2015). Paper-based inkjet-printed microfluidic analytical devices. *Angew. Chem. Int. Ed.* 54, 5294–5310. doi:10.1002/anie.201411508

Zhang, L., Donga, S., and Zhu, L. (2007). Fluorescent dyes of the esculetin and alizarin families respond to zinc ions ratiometrically. *Chem. Commun.* 1891–1893. doi:10.1039/B618413H

Zhang, Z., Hamedpour, V., Lyu, X., Sasaki, Y., and Minami, T. (2021). A printed paper-based anion sensor array for multi-analyte classification: On-site quantification of glyphosate. *ChemPlusChem* 86, 798–802. doi:10.1002/cplu.202100041